A measurement-device-independent quantum key distribution protocol with a heralded single photon source*

ZHOU Yuan-yuan (周媛媛)**, **ZHOU Xue-jun** (周学军), **and SU Bin-bin** (苏彬彬)
Electronic Engineering College, Naval University of Engineering, Wuhan 430033, China

(Received 25 December 2015)

With a heralded single photon source (HSPS), a measurement-device-independent quantum key distribution (MDI-QKD) protocol is proposed, combined with a three-intensity decoy-state method. HSPS has the two-mode characteristic, one mode is used as signal mode, and the other is used as heralded mode to reduce the influence of the dark count. The lower bound of the yield and the upper bound of the error rate are deduced and the performance of the MDI-QKD protocol with an HSPS is analyzed. The simulation results show that the MDI-QKD protocol with an HSPS can achieve a key generation rate and a secure transmission distance which are close to the theoretical limits of the protocol with a single photon source (SPS). Moreover, the key generation rate will improve with the raise of the senders' detection efficiency. The key generation rate of the MDI-QKD protocol with an HSPS is a little less than that of the MDI-QKD protocol with a weak coherent source (WCS) in the close range, but will exceed the latter in the far range. Furthermore, a farther transmission distance is obtained due to the two-mode characteristic of HSPS.
Document code: A **Article ID:** 1673-1905(2016)02-0148-4
DOI 10.1007/s11801-016-5275-3

Quantum key distribution (QKD)[1] has drawn considerable attention as a method of achieving a shared unconditional secure private key. The theoretical and experimental studies have obtained remarkable results[2-6]. However, the setups used in the practical system are imperfect, which will threaten the security of the practical QKD. Photon number splitting (PNS)[7] attack made people realize the loophole left by the imperfect optical source. Fortunately, the decoy-state method[8] was proposed to be a very useful candidate for substantially resisting the PNS attack and enhancing the performance of QKD. Similarly, due to the imperfection of measurement devices, a variety of loopholes were used by Eve to attack QKD, such as a time-shift attack[9], detector-blinding attack[10], faked states attack[11], and so on. In 2012, Lo et al presented a protocol of measurement-device-independent quantum key distribution (MDI-QKD)[12] to exclude all these attacks on detectors. Recently, it has become the most efficient and prominent method to bring MDI-QKD and decoy states together for a better security and performance. Refs.[13—17] analyzed the transmission distance, statistical fluctuation, parameter optimization, etc. Liu[18] and Tang[19] implemented the phase encoding and polarization encoding MDI-QKD. Pan Jian-wei and his team[20] implemented MDI-QKD with 200 km transmission distance for the first time.

However, the above studies are all based on weak coherent sources (WCSs). This paper will consider another optical source, namely the heralded single photon source (HSPS)[21-24], which is frequently used in the normal QKD experiments. We will propose a new MDI-QKD method with three intensity states (signal state, vacuum state and decoy state), and analyze the performance in detail.

The state of the photons generated in two modes by HSPS can be written as

$$|\psi\rangle=\sum_{n=0}^{\infty}\sqrt{P_n}\,|n\rangle|n\rangle\,, \tag{1}$$

where $|n\rangle$ represents an n-photon state, $P_n=x^n/(1+x)^{n+1}$ is the probability to get an n-photon pair and x is the intensity of one mode. The photon number of two modes is always the same.

The system model for the HSPS MDI-QKD with polarization encoding method and BB84 protocol is shown as Fig.1. Alice and Bob both generate two-mode signals. One mode is used as signal mode to be encoded in x or y basis by a polarization modulator (Pol-M). After intensity modulation, the signal mode is sent to the third party who will perform a Bell state measurement (BSM) and announce his results. Alice and Bob can distill a secret key by performing error correction and private amplification. The other mode is detected by the detector a_0 or b_0 to forecast the photon number and arrival time of the relevant signal mode. The method will reduce the influence of dark count on the QKD in long distance.

* This work has been supported by the National Natural Science Foundation of China (No.61302099).
** E-mail: zyy_hjgc@aliyun.com

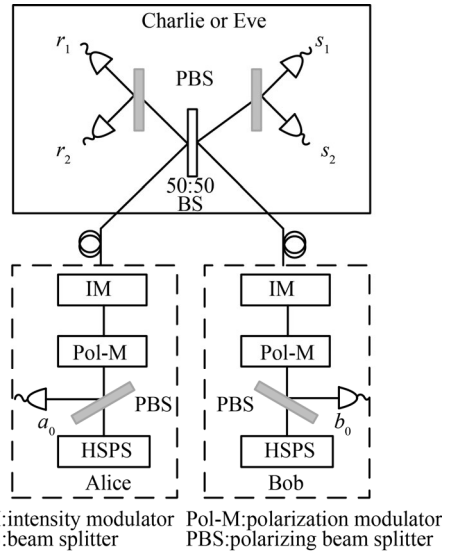

Fig.1 The system model for HSPS MDI-QKD

We design the MDI-QKD protocol as follows.

(1) Alice and Bob both generate three kinds of pulses with different intensities randomly: vacuum state, decoy state and signal state, denoted as u_0, u_1, u_2 (Alice) and v_0, v_1, v_2 (Bob), respectively, which satisfy $u_2>u_1>u_0=0$, $v_2>v_1>v_0=0$.

(2) We suppose that Alice and Bob use threshold detectors which can only tell whether there is photon or not. The detecting result is defined as j, where $j=0$ indicates that the detector is not untriggered and $j=1$ indicates that the detector is triggered. Given an incoming i-photon state, the probability of the detecting result is defined as η_j given by

$$\eta_j=\left[(1-P_{\mathrm{d}})(1-\eta_{\mathrm{d}})^i\right]^{(1-j)}\left[1-(1-P_{\mathrm{d}})(1-\eta_{\mathrm{d}})^i\right]^j, \tag{2}$$

where P_{d} and η_{d} are the dark count rate and detection efficiency of the detector, respectively. We suppose the parameters of all detectors are the same.

Then we define Q_{uv} and E_{uv} to be the overall rate and the quantum bit error rate (*QBER*), respectively, when the intensity of the pulse from Alice is u and that from Bob is v.

$$Q_{uv}^{\omega,j_{\mathrm{A}},j_{\mathrm{B}}}=\sum_{n,m=0}^{\infty}\frac{u^n v^m}{(1+u)^{n+1}(1+v)^{m+1}}\eta_{j_{\mathrm{A}}}\eta_{j_{\mathrm{B}}}Y_{nm}^{\omega}, \tag{3}$$

$$E_{uv}^{\omega,j_{\mathrm{A}},j_{\mathrm{B}}}Q_{uv}^{\omega,j_{\mathrm{A}},j_{\mathrm{B}}}=\sum_{n,m=0}^{\infty}\frac{u^n v^m}{(1+u)^{n+1}(1+v)^{m+1}}\eta_{j_{\mathrm{A}}}\eta_{j_{\mathrm{B}}}e_{nm}^{\omega}Y_{nm}^{\omega}, \tag{4}$$

where $\omega=x$ or z. Alice and Bob estimate the parameters of channel in the x basis and distill the secure key in the z basis. Y_{nm}^{ω} is the probability to obtain a successful BSM when Alice sends an n-photon state and Bob sends an m-photon state. e_{nm}^{ω} is the corresponding error probability. j_{A} and j_{B} correspond to Alice's and Bob's detecting results. Just as Eqs.(3) and (4), Q_{uv} and E_{uv} can be divided into four events respectively according to the different values of j_{A} and j_{B}: $Q_{uv}^{\omega,1,1}$ and $E_{uv}^{\omega,1,1}$ are defined as triggered events, while $Q_{uv}^{\omega,0,0}$ and $E_{uv}^{\omega,0,0}$ are defined as untriggered events.

(3) When both detectors a_0 and b_0 are triggered, the third party performs BSM, that is, Alice and Bob only use triggered events to generate key to reduce the influence of dark count on QKD in long distance. The final key generation rate is given by

$$R\geq\frac{u_2v_2}{(1+u_2)^2(1+v_2)^2}Y_{11}^{z}\left[1-H\left(e_{11}^{x}\right)\right]-Q_{u_2v_2}^{z,1,1}f\left(E_{u_2v_2}^{z,1,1}\right)H\left(E_{u_2v_2}^{z,1,1}\right), \tag{5}$$

where $f(x)$ is the bidirectional error correction efficiency. $H_2(x)$ is the binary Shannon information entropy function given by $H_2(x)=-x\log_2(x)-(1-x)\log_2(1-x)$. $Q_{u_2v_2}^{z,1,1}$ and $E_{u_2v_2}^{z,1,1}$ can be observed in the experiment. In order to calculate the final key generation rate, we need to estimate the lower bound of Y_{11}^{z} and the upper bound of e_{11}^{x}.

We notice that Eqs.(3) and (4) are independent of the basis choice, so we neglect the superscript ω in the following derivation. From Eq.(3), we can get

$$\begin{aligned}&(1+u)(1+v)Q_{uv}^{1,1}=\\&\sum_{n,m=0}^{\infty}\frac{u^n v^m}{(1+u)^n(1+v)^m}\left[1-(1-\eta_{\mathrm{d}})^n\right]\left[1-(1-\eta_{\mathrm{d}})^m\right]Y_{nm}=\\&\sum_{m=0}^{\infty}\frac{v^m P_{\mathrm{d}}}{(1+v)^m}\left[1-(1-\eta_{\mathrm{d}})^m\right]Y_{0m}+\frac{u\eta_{\mathrm{d}}}{1+u}\left\{P_{\mathrm{d}}Y_{10}+\frac{v\eta_{\mathrm{d}}}{1+v}Y_{11}+\right.\\&\left.\sum_{m=2}^{\infty}\frac{v^m}{(1+v)^m}\left[1-(1-\eta_{\mathrm{d}})^m\right]Y_{1m}\right\}+\sum_{n=2}^{\infty}\frac{u^n}{(1+u)^n}\left[1-(1-\eta_{\mathrm{d}})^n\right]\times\\&\left\{P_{\mathrm{d}}Y_{n0}+\frac{v\eta_{\mathrm{d}}}{1+v}Y_{n1}+\sum_{m=2}^{\infty}\frac{v^m}{(1+v)^m}\left[1-(1-\eta_{\mathrm{d}})^m\right]Y_{nm}\right\}=\\&(1+v)Q_{0v}^{1,1}+\frac{uv\eta_{\mathrm{d}}^2}{(1+u)(1+v)}Y_{11}+\\&(1+u)Q_{u0}^{1,1}-Q_{00}^{1,1}+h(u,v),\end{aligned} \tag{6}$$

where

$$\begin{aligned}h(u,v)=&\sum_{m=2}^{\infty}\frac{\eta_{\mathrm{d}}uv^m}{(1+u)(1+v)^m}\left[1-(1-\eta_{\mathrm{d}})^m\right]Y_{1m}+\\&\sum_{n=2}^{\infty}\frac{\eta_{\mathrm{d}}vu^n}{(1+v)(1+u)^n}\left[1-(1-\eta_{\mathrm{d}})^n\right]Y_{n1}+\\&\sum_{n,m=2}^{\infty}\frac{u^n v^m}{(1+u)^n(1+v)^m}\left[1-(1-\eta_{\mathrm{d}})^n\right]\left[1-(1-\eta_{\mathrm{d}})^m\right]Y_{nm}.\end{aligned} \tag{7}$$

We can estimate the lower bound of Y_{11} with $Q_{u_2v_2}^{1,1}$ and $Q_{u_1v_1}^{1,1}$.

$$\begin{aligned}&(1+u_2)(1+v_2)Q_{u_2v_2}^{1,1}-(1+u_1)(1+v_1)Q_{u_1v_1}^{1,1}=\\&g_1+\left[\frac{u_2v_2\eta_{\mathrm{d}}^2}{(1+u_2)(1+v_2)}-\frac{u_1v_1\eta_{\mathrm{d}}^2}{(1+u_1)(1+v_1)}\right]Y_{11}+\\&\sum_{m=2}^{\infty}\left\{\eta_{\mathrm{d}}\left[1-(1-\eta_{\mathrm{d}})^m\right]\times\right.\\&\left.\left[\frac{u_2v_2^m}{(1+u_2)(1+v_2)^m}-\frac{u_1v_1^m}{(1+u_1)(1+v_1)^m}\right]Y_{1m}\right\}+\end{aligned}$$

$$\sum_{n=2}^{\infty}\left\{\eta_{\mathrm{d}}\left[1-\left(1-\eta_{\mathrm{d}}\right)^{n}\right]\times\left[\frac{v_2u_2^n}{\left(1+v_2\right)\left(1+u_2\right)^n}-\frac{v_1u_1^n}{\left(1+v_1\right)\left(1+u_1\right)^n}\right]Y_{n1}\right\}+$$

$$\sum_{n,m=2}^{\infty}\left\{\left[1-\left(1-\eta_{\mathrm{d}}\right)^{n}\right]\left[1-\left(1-\eta_{\mathrm{d}}\right)^{m}\right]\left[\frac{u_2^nv_2^m}{\left(1+u_2\right)^n\left(1+v_2\right)^m}-\frac{u_1^nv_1^m}{\left(1+u_1\right)^n\left(1+v_1\right)^m}\right]Y_{nm}\right\}\geq$$

$$g_1+\left[\frac{u_2v_2\eta_{\mathrm{d}}^2}{\left(1+u_2\right)\left(1+v_2\right)}-\frac{u_1v_1\eta_{\mathrm{d}}^2}{\left(1+u_1\right)\left(1+v_1\right)}\right]Y_{11}+$$

$$\alpha\left[h\left(u_2,v_1\right)+h\left(u_1,v_2\right)\right]=$$

$$g_1+g_2+g_3-\left[\frac{\alpha u_2v_1\eta_{\mathrm{d}}^2}{\left(1+u_2\right)\left(1+v_1\right)}+\frac{\alpha u_1v_2\eta_{\mathrm{d}}^2}{\left(1+u_1\right)\left(1+v_2\right)}-\frac{u_2v_2\eta_{\mathrm{d}}^2}{\left(1+u_2\right)\left(1+v_2\right)}+\frac{u_1v_1\eta_{\mathrm{d}}^2}{\left(1+u_1\right)\left(1+v_1\right)}\right]Y_{11}, \tag{8}$$

where we use the fact that for any n, $m\geq 2$, the following inequalities always hold, which are given by

$$\frac{v_2^mu_2\left(1+v_1\right)^m\left(1+u_1\right)-v_1^mu_1\left(1+v_2\right)^m\left(1+u_2\right)}{v_1^mu_2\left(1+v_2\right)^m\left(1+u_1\right)+v_2^mu_1\left(1+v_1\right)^m\left(1+u_2\right)}\geq$$

$$\frac{v_2^2u_2\left(1+v_1\right)^2\left(1+u_1\right)-v_1^2u_1\left(1+v_2\right)^2\left(1+u_2\right)}{v_1^2u_2\left(1+v_2\right)^2\left(1+u_1\right)+v_2^2u_1\left(1+v_1\right)^2\left(1+u_2\right)}=a\geq 0,$$

$$\frac{v_2u_2^n\left(1+v_1\right)\left(1+u_1\right)^n-v_1u_1^n\left(1+v_2\right)\left(1+u_2\right)^n}{v_1u_2^n\left(1+v_2\right)\left(1+u_1\right)^n+v_2u_1^n\left(1+v_1\right)\left(1+u_2\right)^n}\geq$$

$$\frac{v_2u_2^2\left(1+v_1\right)\left(1+u_1\right)^2-v_1u_1^2\left(1+v_2\right)\left(1+u_2\right)^2}{v_1u_2^2\left(1+v_2\right)\left(1+u_1\right)^2+v_2u_1^2\left(1+v_1\right)\left(1+u_2\right)^2}=b\geq 0,$$

$$\frac{v_2^mu_2^n\left(1+v_1\right)^m\left(1+u_1\right)^n-v_1^mu_1^n\left(1+v_2\right)^m\left(1+u_2\right)^n}{v_1^mu_2^n\left(1+v_2\right)^m\left(1+u_1\right)^n+v_2^mu_1^n\left(1+v_1\right)^m\left(1+u_2\right)^n}\geq$$

$$\frac{v_2^2u_2^2\left(1+v_1\right)^2\left(1+u_1\right)^2-v_1^2u_1^2\left(1+v_2\right)^2\left(1+u_2\right)^2}{v_1^2u_2^2\left(1+v_2\right)^2\left(1+u_1\right)^2+v_2^2u_1^2\left(1+v_1\right)^2\left(1+u_2\right)^2}=c\geq 0, \tag{9}$$

where $\alpha=\min\{a, b, c\}$.

$$g_1=\left(1+v_2\right)Q_{0v_2}^{1,1}-\left(1+v_1\right)Q_{0v_1}^{1,1}+\left(1+u_2\right)Q_{u_20}^{1,1}-\left(1+u_1\right)Q_{u_10}^{1,1}-Q_{00}^{1,1},$$

$$g_2=\alpha\left[\left(1+u_2\right)\left(1+v_1\right)Q_{u_2v_1}^{1,1}-\left(1+v_1\right)Q_{0v_1}^{1,1}-\left(1+u_2\right)Q_{u_20}^{1,1}+Q_{00}^{1,1}\right],$$

$$g_3=\alpha\left[\left(1+u_1\right)\left(1+v_2\right)Q_{u_1v_2}^{1,1}-\left(1+v_2\right)Q_{0v_2}^{1,1}-\left(1+u_1\right)Q_{u_10}^{1,1}+Q_{00}^{1,1}\right]. \tag{10}$$

According to Eq.(8), the lower bound of Y_{11} is given by

$$Y_{11}^{\omega}\geq\frac{g_1+g_2+g_3-\left(1+u_2\right)\left(1+v_2\right)Q_{u_2v_2}^{1,1}+\left(1+u_1\right)\left(1+v_1\right)Q_{u_1v_1}^{1,1}}{\frac{\alpha u_2v_1\eta_{\mathrm{d}}^2}{\left(1+u_2\right)\left(1+v_1\right)}+\frac{\alpha u_1v_2\eta_{\mathrm{d}}^2}{\left(1+u_1\right)\left(1+v_2\right)}-\frac{u_2v_2\eta_{\mathrm{d}}^2}{\left(1+u_2\right)\left(1+v_2\right)}+\frac{u_1v_1\eta_{\mathrm{d}}^2}{\left(1+u_1\right)\left(1+v_1\right)}}. \tag{11}$$

Subsequently, we estimate the upper bound of e_{11}. According to Eq.(4), we have

$$\left(1+u_1\right)\left(1+v_1\right)Q_{u_1v_1}^{1,1}E_{u_1v_1}^{1,1}=g_4+\frac{u_1v_1\eta_{\mathrm{d}}^2}{\left(1+u_1\right)\left(1+v_1\right)}Y_{11}e_{11}+h'\left(u_1,v_1\right), \tag{12}$$

where

$$g_4=\left(1+v_1\right)Q_{0v_1}^{1,1}E_{0v_1}^{1,1}+\left(1+u_1\right)Q_{u_10}^{1,1}E_{u_10}^{1,1}-Q_{00}^{1,1}E_{00}^{1,1}, \tag{13}$$

$$h'\left(u_1,v_1\right)=\sum_{m=2}^{\infty}\left\{\frac{\eta_{\mathrm{d}}u_1v_1^m}{\left(1+u_1\right)\left(1+v_1\right)^m}\left[1-\left(1-\eta_{\mathrm{d}}\right)^{m}\right]Y_{1m}e_{1m}\right\}+\sum_{n=2}^{\infty}\left\{\frac{\eta_{\mathrm{d}}v_1u_1^n}{\left(1+v_1\right)\left(1+u_1\right)^n}\left[1-\left(1-\eta_{\mathrm{d}}\right)^{n}\right]Y_{n1}e_{n1}\right\}+\sum_{n,m=2}^{\infty}\left\{\frac{u_1^nv_1^m}{\left(1+u_1\right)^n\left(1+v_1\right)^m}\left[1-\left(1-\eta_{\mathrm{d}}\right)^{n}\right]\left[1-\left(1-\eta_{\mathrm{d}}\right)^{m}\right]Y_{nm}e_{nm}\right\} \tag{14}$$

Thus, the upper bound of e_{11} is given by

$$e_{11}^{\omega}\leq\frac{\left(1+u_1\right)^2\left(1+v_1\right)^2Q_{u_1v_1}^{1,1}E_{u_1v_1}^{1,1}-\left(1+u_1\right)\left(1+v_1\right)g_4^{\omega}}{u_1v_1\eta_{\mathrm{d}}^2Y_{11}}. \tag{15}$$

Now, we can calculate the final key rate with Eqs.(5), (11) and (15). We use the parameters mainly from Ref.[14]. $P_{\mathrm{d}}=3\times10^{-6}$, $e_{\mathrm{d}}=1.5\%$, $\eta_{\mathrm{d}}=0.3$, $f=1.16$, and the channel loss is α=0.21 dB/km. In simulation, for the decoy states, u_1=v_1=0.01. The signal states u_2 and v_2 are optimized at each distance value.

Fig.2 shows that the key generation and secure transmission distance of HSPS MDI-QKD are very close to the limits of single photon source (SPS) MDI-QKD, and the HSPS MDI-QKD can obtain an advantage about 20 km in secure transmission distance compared with WCS MDI-QKD. There is a crossover at 239 km. The key generation rate of the HSPS MDI-QKD is a little less than that of WCS MDI-QKD protocol in the close range, but will exceed the latter in the far range. The reason for the gap in front distance is the higher ratio of the multi-photon states in HSPS compared with WCS. But over the crossover, the heralded-photon-number method can reduce the influence of dark count and extend the distance.

We calculate the final key rates of HSPS MDI-QKD with different detection efficiencies on Alice's and Bob's sides respectively (η_{d}=0.9, 0.6, 0.3, 0.1). Fig.3 shows that the performance enhances obviously when η_{d} changes from 0.1 to 0.9. Therefore, the detection efficiency is higher and more

non-vacuum pulses can be detected. In this way, the data in triggered events will increase and the performance of MDI-QKD will be improved finally. Here, we suppose the third party's detection efficiency is constant to observe the influence of Alice's and Bob's detection efficiencies on the performance of HSPS MDI-QKD.

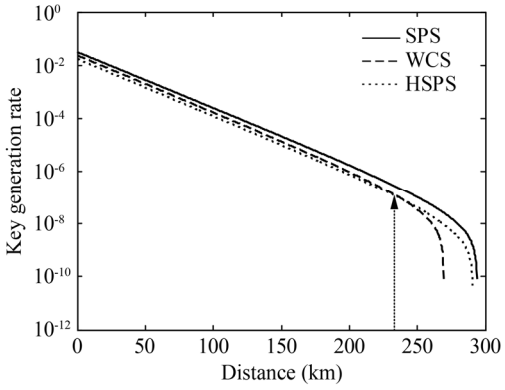

Fig.2 The curves of the key generation rate as a function of the secure transmission distance with different sources

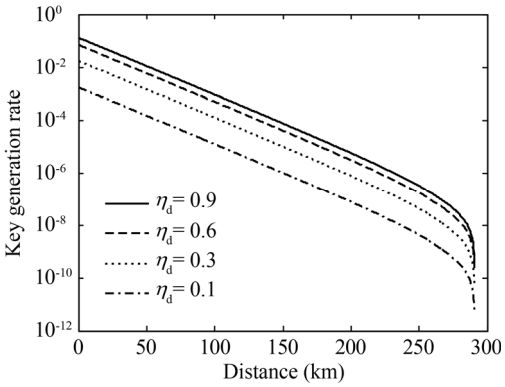

Fig.3 A performance comparison of HSPS MDI-QKD with different detection efficiencies on Alice's and Bob's sides

In summary, an MDI-QKD protocol is proposed combining the three-intensity decoy-state method with an HSPS. The lower bound of the yield and the upper bound of the error rate are deduced and the performance is analyzed through numerical simulation. Firstly, the key generation rate and secure transmission distance of HSPS MDI-QKD are very close to the limits of the SPS MDI-QKD. Secondly, there is a crossover on the performance curves of HSPS MDI-QKD and WCS MDI-QKD. The key generation rate of the HSPS MDI-QKD is a little less than that of WCS MDI-QKD in the close range, but will exceed the latter in the far range. Thirdly, the HSPS MDI-QKD can obtain longer transmission distance than the WCS MDI-QKD. Finally, the performance enhances obviously when the detection efficiencies of senders' detectors rise. Therefore, the HSPS MDI-QKD protocol is effective and feasible.

References

[1] C. H. Bennett and G. Brassard, Quantum Cryptography: Public Key Distribution and Coin Tossing, in Proceedings of IEEE International Conference on Computers, Syetems and Signal Processing, Bangalore, India, 1984.

[2] Y. Y. Zhou, H. Q. Zhang, X. J. Zhou and P. G. Tian, Acta Phys. Sin. **62**, 200302 (2013). (in Chinese)

[3] Y. Y. Zhou, X. J. Zhou, P. G. Tian and Y. J. Wang, Chin. Phys. B **22**, 010305 (2013).

[4] Y. Y. Zhou and X. J. Zhou, Acta Phys. Sin. **60**, 100301 (2011). (in Chinese)

[5] Y. Y. Zhou and X. J. Zhou, Optoelectron. Lett. **11**, 0149 (2015).

[6] Q. Wang, W. Chen, G. Xavier, M. Swillo, T. Zhang, S. Sauge, M. Tengner, Z. F. Han, G. C. Guo and A. Karlsson, Phys. Rev. Lett. **100**, 090501 (2008).

[7] X. B. Wang, Phys. Rev. Lett. **94**, 230503 (2005).

[8] W. Y. Hwang, Phys. Rev. Lett. **91**, 057901 (2003).

[9] V. Makarov, New J. Modern Opt. **11**, 065003 (2009).

[10] L. Lars, W Carlos and W Christoffer, Nature Photonics **4**, 686 (2000).

[11] V. Makarov and A. Anisimov, Phys. Rev. A **74**, 022313 (2006).

[12] H. K. Lo, M. Curty and B. Qi, Phys. Rev. Lett. **108**, 130503 (2012).

[13] X. F. Ma and R. Mohsen, Phys. Rev. A **86**, 062319 (2012).

[14] S. H. Sun, M. Gao, C. Y. Li and L. M. Liang, Phys. Rev. A **87**, 052329 (2013).

[15] F. H. Xu, M. Curty, B. Qi and H. K. Lo, New J. Phys. **15**, 113007 (2013).

[16] Y. Z. Shan, S. H. Sun, X. C. Ma, M. S. Jiang, Y. L. Zhou and L. M. Liang, Phys. Rev. A **90**, 042334 (2014).

[17] C. Dong, S. H. Zhao, W. H. Zhao, L. Shi and G. H. Zhao, Acta Phys. Sin. **63**, 030302 (2014). (in Chinese)

[18] Y. Liu, T. Y. Chen, L. J. Wang, H. Lao, G. L. Shentu, J. Wian, K. Cui, H. L. Yin, N. L. Liu, L. Li, X. F. Ma, J. S. Pele, M. M. Fejer, Q. Zhang and J. W. Pan, Phys. Rev. Lett. **111**, 130502 (2013).

[19] Z. Tang, Z. Liao, F. Xu, B. Qi, L. Qian and H. K. Lo, Phys. Rev. Lett. **112**, 190503 (2014).

[20] Y. L. Tang, H. L. Yin, S. J. Chen, Y. Liu, W. J. Zhang, X. Jiang, L. Zhang, J. Wang, L. X. You, J. Y. Guan, D. X. Yang, Z. Wang, H. Liang, Z. Zhang, N. Zhou, X. F. Ma, T. Y. Chen, Q. Zhang and J. W. Pan, Phys. Rev. Lett. **113**, 190501 (2014).

[21] Q. Wang, X. B. Wang and G. C. Guo, Phys. Rev. A **75**, 012312 (2007).

[22] W. Mauerer and C. Silberhorn, Phys. Rev. A **75**, 050305 (2007).

[23] Y. Adachi, T. Yamamoto, M. Koashi and N. Imoto, Phys. Rev. Lett. **99**, 180503 (2007).

[24] Q. Wang, W. Chen, G. Xavier, M. Swillo, T. Zhang, S. Sauge, M. Tengner, Z. F. Han, G. C. Guo and A. Karlsson, Phys. Rev. Lett. **100**, 090501 (2008).